

Article

Influence of the Size and Shape of Halopyridines Guest Molecules G on the Crystal Structure and Conducting Properties of Molecular (Super)Conductors of (BEDT-TTF)₄A⁺[M³⁺(C₂O₄)₃]·G Family

 Tatiana G. Prokhorova ^{1,*}, Eduard B. Yagubskii ^{1,*}, Andrey A. Bardin ^{2,*}, Vladimir N. Zverev ^{3,4}, Gennadiy V. Shilov ¹ and Lev I. Buravov ¹
¹ Institute of Problems of Chemical Physics, Russian Academy of Sciences, 142432 Chernogolovka, Russia; shilg@icp.ac.ru (G.V.S.); buravov@icp.ac.ru (L.I.B.)

² Institute of Microelectronics Technology and High Purity Materials, Russian Academy of Sciences, 142432 Chernogolovka, Russia

³ Institute of Solid State Physics, Russian Academy of Sciences, 142432 Chernogolovka, Russia; zverev@issp.ac.ru

⁴ Moscow Institute of Physics and Technology, 141700 Dolgoprudny, Russia

* Correspondence: prokh@icp.ac.ru (T.G.P.); yagubskii@icp.ac.ru (E.B.Y.); dr.abardin@gmail.com (A.A.B.)



Citation: Prokhorova, T.G.; Yagubskii, E.B.; Bardin, A.A.; Zverev, V.N.; Shilov, G.V.; Buravov, L.I. Influence of the Size and Shape of Halopyridines Guest Molecules G on the Crystal Structure and Conducting Properties of Molecular (Super)Conductors of (BEDT-TTF)₄A⁺[M³⁺(C₂O₄)₃]·G Family. *Magnetochemistry* **2021**, *7*, 83. <https://doi.org/10.3390/magnetochemistry7060083>

Academic Editors: Carlos J. Gómez García, John Wallis, Lee Martin, Scott Turner and Hiroki Akutsu

Received: 3 May 2021

Accepted: 31 May 2021

Published: 4 June 2021

Publisher's Note: MDPI stays neutral with regard to jurisdictional claims in published maps and institutional affiliations.



Copyright: © 2021 by the authors. Licensee MDPI, Basel, Switzerland. This article is an open access article distributed under the terms and conditions of the Creative Commons Attribution (CC BY) license (<https://creativecommons.org/licenses/by/4.0/>).

Abstract: New organic (super)conductors of the β''-(BEDT-TTF)₄A⁺[M³⁺(C₂O₄)₃]G family, where BEDT-TTF is bis(ethylenedithio)tetrathiafulvalene; M is Fe; A is the monovalent cation NH₄⁺; G is 2-fluoropyridine (2-FPy) (1); 2,3-difluoropyridine (2,3-DFPy) (2); 2-chloro-3-fluoropyridine (2-Cl-3-FPy) (3); 2,6-dichloropyridine (2,6-DClPy) (4); 2,6-difluoropyridine (2,6-DFPy) (5), have been prepared and their crystal structure and transport properties were studied. All crystals have a layered structure in which the conducting layers of BEDT-TTF radical cations alternate with paramagnetic supramolecular anionic layers {A⁺[Fe³⁺(C₂O₄)₃]³⁻G⁰}²⁻. Crystals **1** undergo a structural phase transition from the monoclinic (C2/c) to the triclinic (P $\bar{1}$) symmetry in the range 100–150 K, whereas crystals **2–5** have a monoclinic symmetry in the entire range of the X-ray experiment (100–300 K). The alternating current (ac) conductivity of salts **1–4** exhibits metallic behavior down to 1.4 K, whereas the salt **5** demonstrates the onset of a superconducting transition at 3.1 K. The structures and conducting properties of **1–5** are compared with those of the known monoclinic phases of the family containing different monohalopyridines as “guest” solvent molecules G.

Keywords: BEDT-TTF; molecular paramagnetic (super)conductors; radical cation salts; tris(oxalato)metallate anions

1. Introduction

The large family of layered molecular (super)conductors (BEDT-TTF)₄A⁺[M³⁺(C₂O₄)₃]G, where BEDT-TTF is bis(ethylenedithio)tetrathiafulvalene; M³⁺ is a magnetic or non-magnetic metal cation (M = Fe, Cr, Mn, Ru, Rh, Ga, Co, Al); G is a neutral “guest” molecule; A⁺ is a small monovalent cation (A⁺ = NH₄⁺, K⁺, H₃O⁺, Rb⁺), continues to be actively investigated [1–29]. This is due to the fact that structural and conducting properties of this four-component system can be widely modified by changing the components A⁺, M³⁺ and G. All crystals have a layered structure in which the conducting radical cation layers of BEDT-TTF alternate with insulating supramolecular anionic layers {A⁺[M³⁺(C₂O₄)₃]³⁻G⁰}²⁻. Cationic and anionic layers interact with each other through the formation of a large number of hydrogen bonds between the components of the anionic layer and terminal ethylene groups of BEDT-TTF. The anionic layers have a familiar honeycomb-like structure in which M³⁺ and A⁺ cations linked by oxalate bridges form the hexagonal cavities in which neutral “guest” molecules G are incorporated. Cationic layers have different BEDT-TTF packing types depending on the chemical composition of the anionic layers.

The main feature of $(\text{BEDT-TTF})_4\text{A}^+[\text{M}^{3+}(\text{C}_2\text{O}_4)_3]\text{G}$ crystals is that the crystal symmetry, packing type of conducting BEDT-TTF layers, and therefore, the conducting properties of crystals depend mainly on the size and shape of the included “guest” molecule G [1,3,17–20]. The variation of M (keeping the G the same) leads to a noticeable change of conducting properties, but does not affect the crystal symmetry and the type of packing of cation layers. The nature of the singly charged cation A^+ affects the properties of the crystals weakly. Currently, four groups of $(\text{BEDT-TTF})_4\text{A}^+[\text{M}^{3+}(\text{C}_2\text{O}_4)_3]\text{G}$ crystals are known, which have different symmetry and BEDT-TTF packing type.

The largest and more interesting group of this family is the group of monoclinic ($\text{C}2/c$) crystals [1–17,19,21,23–28] with β'' -packing type of BEDT-TTF, according to the structural classification of salts of BEDT-TTF and its analogues [30,31]. The β'' -layers are composed of continuous stacks of radical cations, the planes of which are almost parallel and shifted with respect to the short axis of the BEDT-TTF molecule. The interplanar distances in the stacks are considerably shortened in comparison with the normal van der Waals distances. There are a large number of shortened S S contacts between adjacent stacks in the layer.

Monoclinic β'' - $(\text{BEDT-TTF})_4\text{A}^+[\text{M}^{3+}(\text{C}_2\text{O}_4)_3]\text{G}$ crystals were obtained with a large number of guest molecules G (G = PhCN, PhNO₂, PhBr, PhCl, PhF, PhI, DMF, py, CH₂Cl₂, 1,2-dichloro- and 1,2-dibromobenzene, different isomers of halopyridines). The conducting properties of these crystals vary from semiconducting to metallic and superconducting depending on the size, shape, and orientation of G in the hexagonal cavity, while the dimensions of the hexagonal cavity weakly depend on the size of G and are determined by the size of the M^{3+} cation and the distance from the outer oxalate oxygen atoms to the cation A^+ . As a result, the large molecules G occupy almost the entire volume of the cavity and their position is strictly fixed. The smaller molecules G can occupy different positions. This leads to an increase in the structural disorder in the anionic layers and terminal ethylene groups of BEDT-TTF and to the suppression of the conductivity of molecular crystals. It was shown later that the conductivity of these crystals depends not so much on the molecular volume of G, as on its length along the direction c of the unit cell, [17]. Not so long ago, a correlation between the value of the c parameter of the unit cell and conducting properties of BEDT-TTF crystals with tris(oxalato)metallate anions was found [29].

The majority of these crystals keep the monoclinic symmetry in the entire range of the X-ray experiment (90–300 K). An exception is several β'' - $(\text{BEDT-TTF})_4(\text{NH}_4^+)[\text{Fe}(\text{C}_2\text{O}_4)_3]\text{G}$ crystals containing PhHal (Hal = F, Cl, Br) or a mixture of PhHal with PhCN as G. In these crystals, the superconducting transition is preceded by a structural phase transition from the monoclinic to triclinic state with decreasing temperature [21,22,25]. This structural transition arises from noticeable positional shifts of all components of the complex anion, giving rise to two nonequivalent organic β'' -layers and the partial ordering of the ethylene groups of BEDT-TTF molecules. The consequence of these changes is the phase transitions of these crystals from metallic to mixed metallic/insulating states [32]. According to the theoretical concepts of Merino and McKenzie, the appearance of this state precedes the appearance of superconductivity in layered molecular conductors with a quarter-filled conduction band [33]. All of the aforementioned crystals containing PhHal as G support this conclusion.

In addition to β'' -monoclinic crystals, three more groups of crystals were discovered in the $(\text{BEDT-TTF})_4\text{A}^+[\text{M}^{3+}(\text{C}_2\text{O}_4)_3]\text{G}$ family: orthorhombic crystals (space group $Pbcn$) with “pseudo- k'' ”-type of BEDT-TTF-packing [1,4,19,23,27] and bi-layered triclinic crystals (space group $P\bar{1}$) in the structure in which conducting layers with α - and β'' - or α - and “pseudo- κ'' ”-types of BEDT-TTF packing alternate [11,20,24].

The group of orthorhombic “pseudo- k'' ”-crystals includes several semiconducting crystals (M = Fe, Cr, Co, Al; $\text{A}^+ = \text{K}^+, \text{NH}_4^+, \text{H}_3\text{O}^+$; G = PhCN and its mixtures with PhNO₂ or C₆H₄Cl₂) [1,4,19]. These crystals grow in “dry” solvents G and also together with monoclinic crystals in the presence of traces of water in the reaction medium. The organic layer of these crystals is formed by charged $[(\text{BEDT-TTF})_2]^{2+}$ dimers surrounded

by neutral [BEDT-TTF] molecules that are perpendicular to the dimers. Due to the strong localization of a charge on dimers, all orthorhombic crystals are semiconductors.

Triclinic crystals are formed with large unsymmetrical (including chiral) solvent molecules (M/G = Fe/PhAc; Fe/(X)-PhCH(OH)Me, X = R/S (racemate) or S (enantiomer); Ga/PhN(Me)CHO; Ga/BnCN; Fe/C₆H₄Br₂, Ga/C₆H₄Br₂) [11,18–20,24]. Bulky unsymmetrical solvent molecules are arranged asymmetrically relative to neighboring conducting layers and interact with them in different ways. For this reason, in the structure of triclinic crystals, conducting layers alternate with two different packing types, α - β'' - or α -“pseudo- κ ”. In the α -layer, the stacks of BEDT-TTF are inclined to one another. Triclinic α -“pseudo- κ ”-crystals are metals down to low helium temperatures, while triclinic α - β'' -crystals undergo a metal-semiconductor transition with decreasing temperature.

Despite the large number of investigations of the influence of guest molecules G on the crystals and conducting properties of family crystals, these studies are ongoing and bring interesting results. In our recent articles, we have reported on the synthesis of crystals containing Fe, Cr, Ga as M and various isomers of monohalopyridines (HalPy) as G in which the halogen atom occupied different positions with respect to the nitrogen atom of the pyridine ring [25,28]. It was shown that the conducting and structural properties of the resulting β'' -(BEDT-TTF)₄A⁺[Fe³⁺(C₂O₄)₃](HalPy) crystals strongly depend on the position of the halogen atom in the pyridine ring and also on the nature of M (see Table 1).

Table 1. Structural and conducting properties of the β'' -(BEDT-TTF)₄A⁺[M³⁺(C₂O₄)₃]-G crystals, where G is HalPy; M is Fe, Cr, Ga; A = H₃O⁺, [K_{0.8}(H₃O)_{0.2}]⁺.

G/M	Structural Properties	Conducting Properties	Ref.
2-ClPy/Fe	C2/c to P $\bar{1}$ transition at 215 K	SC, T _c = 2.4–4.0 K	[25]
2-BrPy/Fe	C2/c to P $\bar{1}$ transition at 190 K	SC, T _c = 4.3 K	[25]
3-ClPy/Fe	No structural transition	M > 0.5 K	[25]
3-BrPy/Fe	No structural transition	M > 0.5 K	[25]
2-ClPy/Cr	Incommensurate structure appears upon cooling	M > 0.5 K	[28]
2-BrPy/Cr	Incommensurate structure appears upon cooling	M > 0.5 K	[28]
2-ClPy/Ga	Incommensurate structure appears upon cooling	M > 0.5 K	[28]
2-BrPy/Ga	Incommensurate structure appears upon cooling	M > 0.5 K	[28]

Here, we report the synthesis, crystal structure and transport properties of new monoclinic crystals β'' -(BEDT-TTF)₄(NH₄⁺)[Fe(C₂O₄)₃]G in which various mono- and dihalopyridines are included as G: 2-fluoropyridine (2-FPy) (1), 2,3-difluoropyridine (2,3-DFPy) (2), 2-chloro-3-fluoropyridine (2-Cl-3-FPy) (3), 2,6-dichloropyridine (2,6-DCIPy) (4), 2,6-difluoropyridine (2,6-DFPy) (5).

2. Results and Discussion

2.1. Synthesis

The reaction medium for the growth of (BEDT-TTF)₄A⁺[M³⁺(C₂O₄)₃]G crystal consists of the guest solvent either neat or mixed with other solvents (H₂O, CH₃OH, C₂H₅OH, CH₃CN, etc.) which are usually not incorporated in the structure but have a considerable effect on the electrocrystallization process. In particular, they increase the solubility of the inorganic electrolyte in the guest organic solvent and, hence, enable variation of the current and the donor/electrolyte molar ratio, i.e., parameters that largely determine the crystal structure, growth rate and quality of crystals formed.

For example, in the medium of anhydrous C₆H₅CN, only semiconducting orthorhombic crystals grow, while both orthorhombic and monoclinic superconducting crystals (T_c = 7–8.5 K) in the form of needles were obtained by P. Day et al. using C₆H₅CN with a small addition of water [1]. These were the first superconducting crystals in this large

family. Until now, the T_c of these crystals remains the highest among the crystals of this family. However, usually, only orthorhombic crystals form in this medium. In addition, needle crystals are of poor quality.

Interesting results were obtained by us when we used the mixture of C_6H_5CN with 1,2,4-trichlorobenzene (or 1,3-dibromobenzene) and C_2H_5OH as a reaction medium [19]. The molecules of 1,2,4-trichlorobenzene and 1,3-dibromobenzene do not enter the structure of crystals due to their size (1,2,4-trichlorobenzene) or geometry (1,3-dibromobenzene), but their presence facilitates the formation of high-quality monoclinic crystals. In this case, monoclinic crystals grow in the form of thick plates or parallelepipeds. Unlike most crystals of BEDT-TTF salts, in which the conducting layers are arranged in the plate plane, in these crystals, the conducting layers are perpendicular to this plane.

The addition of 1,2,4-trichlorobenzene to the reaction medium made it possible to obtain high-quality (super)conducting monoclinic crystals where G is 1,2-dichlorobenzene ($M = Fe$), various isomers of monohalopyridines ($Hal = Cl, Br; M = Fe, Cr, Ga$) as well as crystals containing a 4d metal cation ($M^{3+} = Ru^{3+}, G = PhBr$) and crystals containing two guest solvents, β'' -(BEDT-TTF) $_4A[Fe(C_2O_4)_3][(G1)_x(G2)_{1-x}]$, where $G1 =$ benzonitrile, $G2 =$ 1,2-dichlorobenzene, nitrobenzene, fluorobenzene, chlorobenzene, bromobenzene [17,19,23,25,28].

Of note is that in the medium of 1,2,4-trichlorobenzene with acetophenone or chlorobenzene ($G1$) and fluorobenzene ($G2$), the new series of isomorphic crystals with tris(oxalato)metallate anions β'' -(BEDT-TTF) $_2[(H_2O)(NH_4)_2M(C_2O_4)_3]18$ -crown-6 ($M = Rh, Cr, Ru, Ir$) were synthesized by Lee Martin et al. [34–36]. Two of these crystals ($M = Cr, Rh$) are superconductors.

In this work, the new monoclinic β'' -(BEDT-TTF) $_4(NH_4^+)[Fe(C_2O_4)_3](HalPy)$ crystals (1–5) were also obtained by using the mixtures of 1,2,4-trichlorobenzene with different mono- and dihalopyridines as reaction medium (Table 2).

Table 2. The β'' -(BEDT-TTF) $_4(NH_4^+)[Fe(C_2O_4)_3]G$ salts obtained and their properties.

Salts	G	Structural Properties	Conducting Properties
1	2-FPy	$C2/c$ to $P\bar{1}$ transition at 100–150 K	$M > 1.4$ K
2	2,3-DFPy	$C2/c$ no structural transition	$M > 1.4$ K
3	2-Cl-3-FPy	$C2/c$ no structural transition	$M > 1.4$ K
4	2,6-DCIPy	$C2/c$ no structural transition	$M > 1.4$ K
5	2,6-DFPy	$C2/c$ no structural transition	SC, $T_c = 3.1$ K

Note that unlike all previously used guest components G, which are liquids, 2,6-dichloropyridine (crystals 4) is a solid substance. It is possible that some other solids with interesting physical properties can also be included in the structure of the anionic layers for obtaining new multifunctional compounds combining two or more physical properties in the same crystal lattice.

2.2. Structure

Salts 1–5 of common formula β'' -(BEDT-TTF) $_4(NH_4^+)[Fe(C_2O_4)_3](HalPy)$ crystallize in the monoclinic space group $C2/c$, with two crystallographically independent BEDT-TTF (A and B) molecules, half a $[Fe(C_2O_4)_3]^{3-}$ anion, half a NH_4^+ cation, and half a halopyridine guest molecule. The full cell contains two formula units. Salts 1–5 are isostructural with other monoclinic $C2/c$ BEDT-TTF tris(oxalato)metallates packed by β'' type [27,29]. The structure consists of β'' -type packed BEDT-TTF conducting radical cation layers separated by complex insulating anion layers $\{(NH_4^+)[Fe(C_2O_4)_3]^{3-}(HalPy)\}^{2-}$ interleaved along the c axis (Figure 1). Within the layers, BEDT-TTF radical cations form dimerized stacks with

nearly coplanar molecular mean planes, incorporating radical cations expanding in a AABBAABBAABB manner with a shift of around a half of molecular short axis. Radical cations from adjacent stacks are arranged into chains expanding in the same dimerized manner. In the chains, BEDT-TTF radical cations are placed side-by-side and are nearly coplanar (Figure 2).

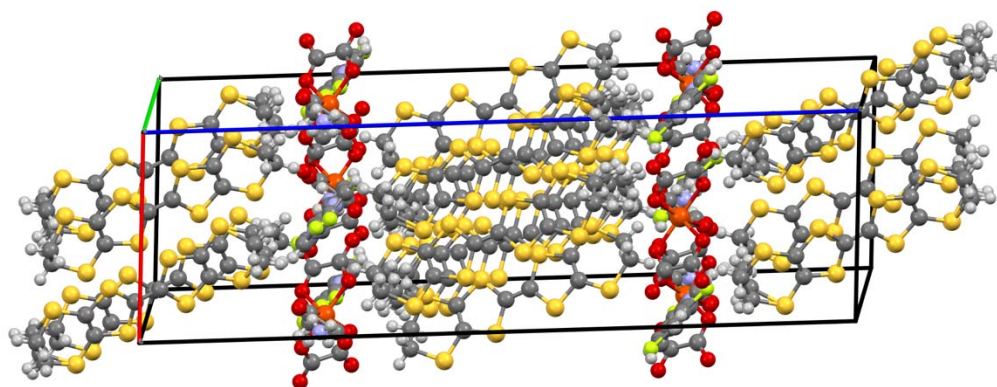


Figure 1. Crystal structure of salt 2 β'' -(BEDT-TTF)₄(NH₄)[Fe(C₂O₄)₃](2,3-DFPy); the other salts are isostructural. Carbon is dark gray, hydrogen is light gray, sulfur is yellow, oxygen is red, nitrogen is light blue, fluorine is light green, and iron is orange.

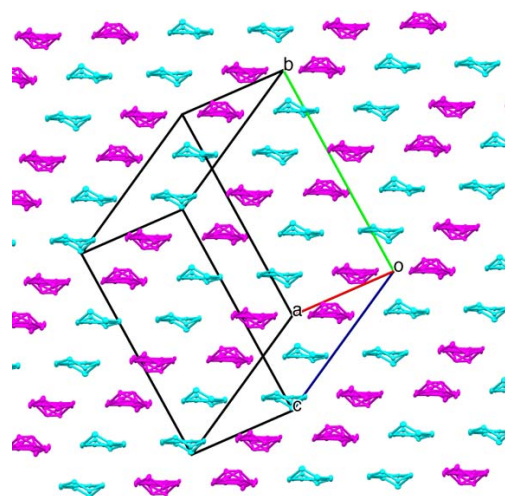


Figure 2. Conducting BEDT-TTF radical cation layers of salts 1–5 packed by β'' -type. Crystallographically unique BEDT-TTF radical cations are denoted by color. Molecule A is colored magenta, B is colored cyan. AABBAABBAABB packing arrangement for BEDT-TTF stacks and chains is shown.

An average charge on the BEDT-TTF is +1/2 obtained from the charge balance requirements. In the salt 5, the radical cation A is completely ordered, both terminal ethylene groups of the radical cation B are disordered over two positions with the occupancies of main positions of 0.61 (atoms C17, C18) and 0.74 (atoms C19, C20) for each terminal correspondingly, Figure S1. Minor positions are complementary to the main positions with the occupancies of 0.39 (atoms C17', C18') and 0.26 (atoms C19', C20'). Mutual arrangements of ethylene groups in a BEDT-TTF respect eclipsed conformation in an ordered molecule A and staggered conformation in a molecule B for both main and minor disordered configurations (Figure 3). The data of the other salts are summarized in Table 3.



Figure 3. Relative positions in a chain and conformations of terminal ethylene groups for independent BEDT-TTF radical cation A (**left**) and B (**right**) in salt 5. Main positions for disordered ethylene groups of B are colored cyan and complementary are colored navy. The conformation is eclipsed for A and staggered for B. Thermal ellipsoids are of 50% probability.

Table 3. BEDT-TTF radical cation terminal ethylene group occupancies and mutual conformation for the salts 1–5. In the case of disordered groups, the occupancies of the main positions are presented. In the case of completely ordered groups, occupancies are equal to unity. Terminal A1 is defined as the ethylene group closest to the Fe^{3+} ion, A2—an opposite side of the molecule. Terminals B1/B2 are defined by the same manner in the relation to the NH^{4+} ion. Letter *e* denotes the eclipsed conformation while *s* denotes the staggered one. An example of *e/s* conformation is presented in Figure 3. Experiment temperature is 100 K unless otherwise noted.

Terminal	1a *	1b *	1c *	2	3	4	5
A1	1/1 [§]	1	1	1	1	1	1
A2	1/1 [§]	1	1	1	1	1	1
B1	1/0.52 ^{&}	0.74	0.63	1	<i>d</i> [#]	1	0.74
B2	0.86/0.63 ^{&}	0.60	0.69	0.69	<i>d</i> [#]	0.62	0.61
A1/A2	<i>e/e</i>	<i>e</i>	<i>e</i>	<i>e</i>	<i>e</i>	<i>e</i>	<i>e</i>
B1/B2	<i>s/s</i>	<i>s</i>	<i>s</i>	<i>e</i>	<i>s</i>	<i>e</i>	<i>s</i>

* 1a = 100 K (triclinic), 1b = 150 K (monoclinic), 1c = 240 K (monoclinic); [#] severe disorder that is unable to be evaluated due to the low quality of the crystal; [§] second value is for molecule C; [&] second value is for molecule D.

It is known that the order and configuration of BEDT-TTF radical cation terminal ethylene groups play an important role in the charge transport of BEDT-TTF-based molecular conductors. From Table 3, it becomes immediately clear that, in all salts 1–5, the molecule A is fully ordered and adopts eclipsed conformation.

Another clear observation is that the configuration of salt 1 at 240 K, and, especially at 150 K, resembles that of 5 at 100 K. Upon cooling in the range 100–150 K, salt 1 experiences a crystal lattice transformation from higher (monoclinic) to lower (triclinic) symmetry. A similar phase transition was observed earlier in the family of halobenzene solvents (PhF, PhCl, PhBr) [21] or their mixtures with PhCN [22] as well as with the guest molecule types closest to the current research—monosubstituted halopyridines, namely, 2-Cl-Py and 2-Br-Py (Table 1). In these cases, the structural transition was associated with a superconductive one. However, no superconductive transition is observed in salt 1. Let us speculate about possible reasons from the perspective of the crystal structure.

The structural transition results in halving of the unit cell volume and appearance of four independent BEDT-TTF radical cations (A, B, C, D). Molecule C is generated from A by the loss of symmetry, and molecule D is generated from B. It is seen from Table 3 that both molecules A and C are still ordered and adopt the same configuration while in the pair B/D the former is almost fully ordered but the latter, in contrast, demonstrates almost randomly distributed occupancies of the terminal group carbon atoms. Such a redistribution of occupancies is most likely accompanied by a charge redistribution that, in turn, results in weak charge localization and loss of superconductive transition. Indeed, analysis of the charge distribution over independent BEDT-TTF radical cations based on bond lengths enables us to roughly estimate the charges on A/B/C/D as +0.5/+0.33/+0.5/+0.67, respectively, indicating a charge redistribution in the pair B/D [37]. This formula, when

applied to the structures with high R -values, often provides wrong absolute values and should not be taken too seriously. However, that gives us a good qualitative insight into the intermolecular charge distribution.

Within each anion layer, the Fe^{3+} and NH_4^+ cations are linked by oxalate bridges forming a hexagonal packing arrangement where Fe^{3+} is octahedrally coordinated by oxalate ligands. Outer oxygens of oxalates form hydrogen bonds with the NH_4^+ cations (Figure 4). This anionic network forms large hexagonal cavities where halopyridine guest molecules reside. Fe^{3+} cations and nitrogen of NH_4^+ cations reside in special positions. There are twofold symmetry axes connecting them.

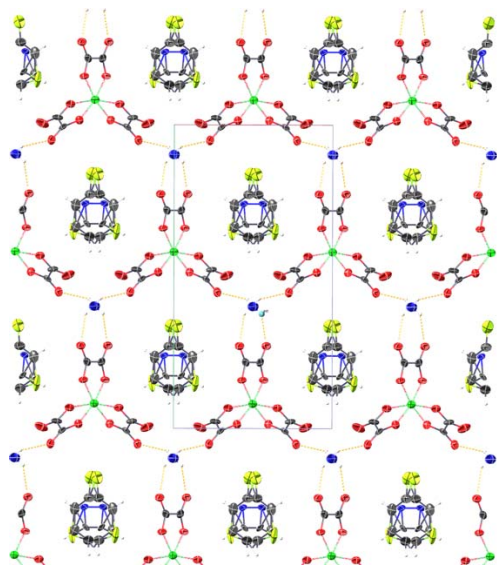


Figure 4. Projection of the anion layer along c axis showing the honeycomb packing arrangement of the tris(oxalato)ferrate anions for the salts 1–5, using salt 5 as an example. Thermal ellipsoids are of 50% probability.

There are two chemically and structurally reasonable alternatives for a cation incorporating into an anion layer—ammonium (NH_4^+) or oxonium (H_3O^+). It should be noted that the unambiguous identification of the cation is a challenging task that has a long history. That is especially a source of doubt for compounds demonstrating superconductive properties, as there is an empirical rule that H_3O^+ favors the superconducting transition [1,27,29].

In the particular case of superconducting salt 5, we consider the cation to be NH_4^+ , guided by the following arguments:

1. Both symmetrically unequivalent hydrogen atoms were found on the electronic differential map;
2. Adding each of the hydrogens results in a subtle but sensible decrease of the R -value;
3. Replacing N by O does not improve the R -value;
4. NH_4^+ cation is residing on a twofold axis and adopts distorted tetrahedral geometry that has been restored to a symmetrical tetrahedron by geometrical constraints without loss of the R -value.

It should be emphasized that, while molecules of 2,6-DFPy and 2,6-DCIPy have their own molecular twofold symmetry axes, they still reside in the cavities with the substantial displacement of approximately 0.8 Å with no atoms occupying special positions, resulting in a positional disorder over two positions around the lattice twofold axis (Table 4, Figures 5 and 6). It is most likely a consequence of the requirement to completely fill up the cavity void space by a smaller molecule. However, the larger chlorine-containing

2,6-DCIPy is almost 0.1 Å less displaced than the fluorine-containing 2,6-DFPy but requires a larger tilt to be accommodated.

Table 4. The dimensions of the anion layer hexagonal cavity and the orientation of the HalPy guest molecule as annotated in Figure 5. δ is the angle between the pyridine ring plane and the plane of the hexagonal cavity. e is a mean guest molecule displacement defined as $(e_1 + e_2)/2$, where e_1 is a displacement of the outer halopyridine halogen atom nearest to the cusp Fe^{3+} ion around the twofold axis, e_2 is a displacement of the inner halopyridine ring carbon/nitrogen atom closest to the nadir nitrogen atom of NH_4^+ ion. e' is an alternative mean displacement value $(e_1 + e_2 + \dots + e_n)/n$ where averaging is taken for all displaced atoms. S is a square unit of the hexagonal cavity taken as $w(b + h)/2$.

Salts	1a	1b	1c	2	3	4	5
$S, \text{\AA}^2$	101.71	102.17	102.850	102.21	101.90	102.03	101.83
$h, \text{\AA}$	13.417	13.453	13.549	13.474	13.463	13.449	13.406
$w, \text{\AA}$	10.298	10.309	10.330	10.331	10.309	10.327	10.322
$a, \text{\AA}$	6.203	6.254	6.291	6.285	6.584	6.277	6.258
$b, \text{\AA}$	6.338	6.370	6.364	6.313	6.306	6.312	6.326
$c, \text{\AA}$	4.625	4.656	4.748	4.484	4.414	4.473	4.813
$d, \text{\AA}$	4.881	5.108	4.969	4.520	4.750	4.535	4.519
$e, \text{\AA}$	0	0	0.651	0.822	0	0.895	0.808
$e', \text{\AA}$	0	0	0.547	0.877	1.108	0.902	0.840
$\delta, ^\circ$	31.73	34.58	34.97	38.14	32.37	39.46	36.36

1a = 100 K (triclinic), 1b = 150 K (monoclinic), 1c = 240 K (monoclinic).

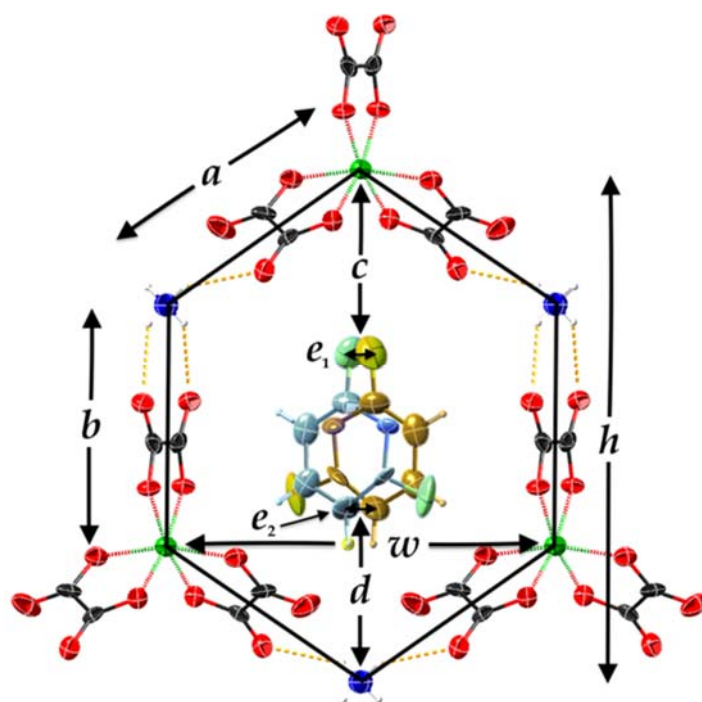


Figure 5. Scheme for the hexagonal unit dimensions and the guest molecule placement in the anion layers of salts 1–5, using salt 5 as an example.

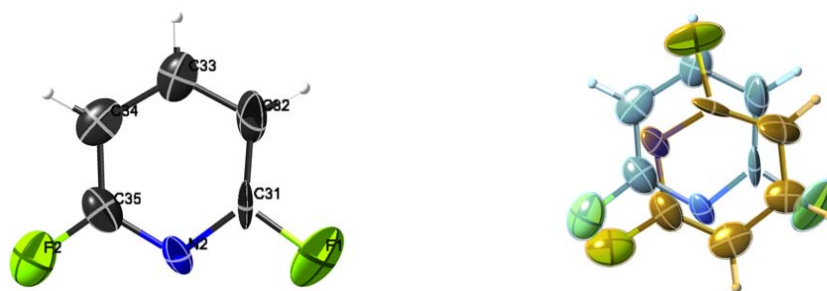


Figure 6. View of the 2,6-DFPy molecule in the crystal structure **5** along the molecular twofold axis (**left**) and along the lattice twofold axis $(-x, y, 1/2 - z)$ (**right**). The 2,6-DCIPy molecule in the crystal structure **4** is arranged in the same manner.

It appears that the smallest 2-FPy guest molecule that lacks any molecular symmetry presents the most interesting case. At higher temperatures, the arrangement of 2-FPy in the cavity resembles 2,6-DFPy/2,6-DCIPy cases with a much smaller displacement. However, upon cooling, the fluorine atom and the two pyridine carbon atoms (C41 and C44) are situated on the lattice twofold axis (Figure 7). This effect is already clear at 150 K—far away from the structural transition. Thus, 2-FPy localization precedes or even induces a complete structural transformation. Nitrogen and carbon positions of 2-FPy appear to be inseparable at temperatures 150 and 100 K; that is probably due to the formation of a domain superstructure. The elevated electric field strength along the domain grains may serve as a factor causing failure of the superconductive transition. However, such speculations require further deeper investigations.

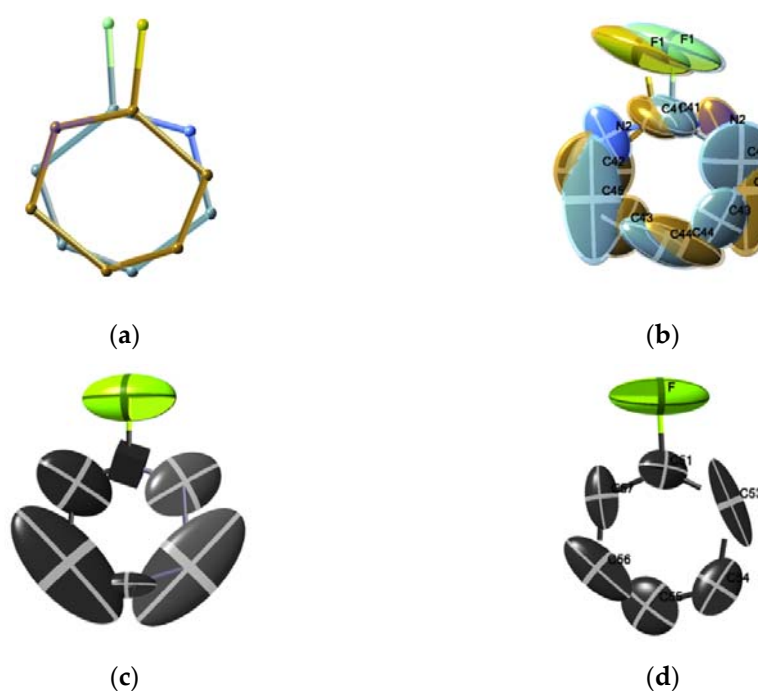


Figure 7. View of 2-FPy molecule in the crystal structure **1**. Wireframe (**a**) and ellipsoid (**b**) views at 240 K (**1c**), 150 K (**1b**) (**c**) and 100 K (**1a**) (**d**). Fluorine and central carbon atoms are placed on lattice twofold axis $(-x, y, 1/2 - z)$ at 150 K.

Unlike all other salts presented in the current work, salt **3**, with the most asymmetrical halopyridine molecule—2-Cl-3-FPy, contains an NH_4^+ cation displaced from the lattice twofold axis and shows an oxalic ligand disorder in the tris(oxalato)ferrate anion (Figure 8). Guest solvent molecules could not be identified by means of crystal structure tools and

were refined as a set of separated carbon atoms plus fluorine with released occupancies. It appears that a highly asymmetric guest solvent molecule with substituents of different sizes does not favor growth of high-quality crystals.

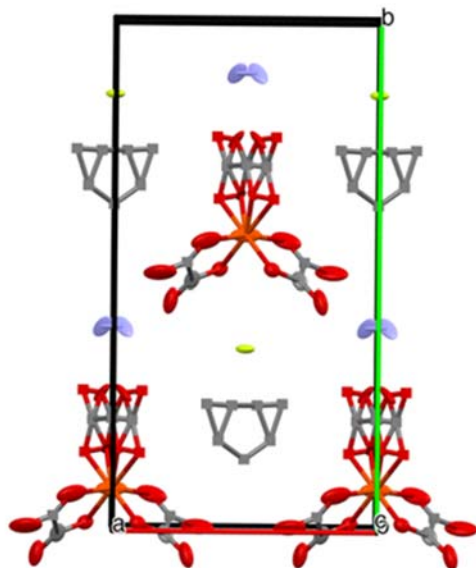


Figure 8. Anion layer of salt 3.

Though the structure-property correlation is a very complex and ambiguous topic, some preliminary conclusions can be provided:

1. Use of highly nonsymmetrical halopyridine 2-Cl-3-FPy leads to low quality single crystals;
2. Guest molecules of higher symmetry and larger volume may produce superconductive single crystals;
3. Ordering of non-symmetrical guest molecules at lower temperatures may impede the SC transition by casting a constant dipole moment at the place of the localization.

2.3. Conducting Properties

The temperature dependences of the out-of-plane resistivity for the samples 1–5 are presented in Figure 9. All these samples are metals despite the existence of the negative slopes on the low-temperature parts on the $\rho_{\perp}(T)$ curves for the samples 5 and 1. Moreover, the sample 5 demonstrates a sharp resistance drop at low temperature which one can surely attribute to the onset of a superconducting transition at $T_c = 3.1$ K. Unfortunately, we could not reach the real zero resistance state, even at our minimal temperature 1.4 K, because the superconducting transition is not very narrow. This is typical for organic metals, for which the transition width is usually more or about 2 K. The behavior of the sample 1 at $T < 20$ K is similar to that of the sample 5, so we do not exclude the possibility that this sample could also be a superconductor at temperatures below 1 K, but we could not check this statement because our temperature region was restricted by 1.4 K.

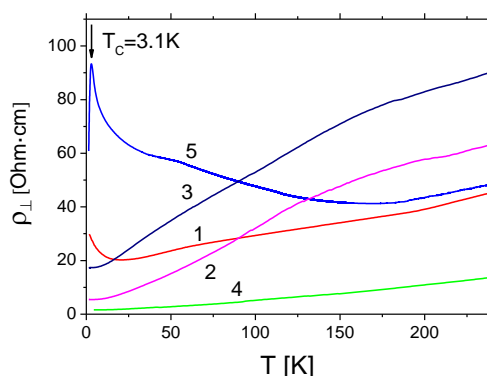


Figure 9. The temperature dependences of the out-of-plane resistivity for the samples 1–5: 2-FPy (1); 2,3-DFPy (2); 2-Cl-3-FPy (3); 2,6-DCIPy (4); 2,6-DFPy (5).

3. Materials and Methods

3.1. Synthesis

Crystals of five new radical cation salts of the β'' -(BEDT-TTF) $_4$ A $^+$ [M $^{3+}$ (C $_2$ O $_4$) $_3$]G family were obtained by electrochemical oxidation of BEDT-TTF at a platinum electrode in organic solvents, at constant current and temperature (25 °C), in the presence of supporting electrolytes, namely, ammonium tris(oxalato)metallates combined with a 18-crown ether. The electrocrystallization process was performed in conventional two-compartment U-shaped cells separated by a porous glass filter. BEDT-TTF, (NH $_4$) $_3$ [Fe(ox) $_3$] \cdot 3H $_2$ O, 18-crown ether and solvents were placed in the cathode compartment and, then, the solution obtained was distributed between the two compartments of the cell.

BEDT-TTF, 1,2,4-trichlorobenzene, 2-fluoropyridine, 2,3-difluoropyridine, 2-chloro-3-fluoropyridine; 2,6-difluoropyridine; 2,6-dichloropyridine, (NH $_4$) $_3$ [Fe(ox) $_3$] \cdot 3H $_2$ O were used as received (Aldrich); 18-crown-6 (Aldrich) was purified by recrystallization from acetonitrile and dried in vacuum at 30 °C over P $_2$ O $_5$.

The exact conditions for the synthesis of each salt are described below.

3.1.1. β'' -(BEDT-TTF) $_4$ (NH $_4^+$)[Fe(ox) $_3$](2-FPy) (1)

15 mg of BEDT-TTF, 150 mg of (NH $_4$) $_3$ [Fe(ox) $_3$] \cdot 3H $_2$ O, 450 mg of 18-crown-6 and the mixture of 2-FPy (10 mL) with 1,2,4-trichlorobenzene (10 mL) and 96% EtOH (2 mL); $J = 0.85 \mu\text{A}$. Many crystals in the form of thick plates were collected from the anode after 9 days.

3.1.2. β'' -(BEDT-TTF) $_4$ (NH $_4^+$)[Fe(ox) $_3$](2,3-DFPy) (2)

8 mg BEDT-TTF, 75 mg of (NH $_4$) $_3$ [Fe(ox) $_3$] \cdot 3H $_2$ O, 250 mg of 18-crown-6 and the mixture of 2,3-DFPy (4 mL) with 1,2,4-trichlorobenzene (4 mL) and 96% EtOH (1 mL); $J = 0.85 \mu\text{A}$. Several thick crystals were collected from the anode after 12 days.

3.1.3. β'' -(BEDT-TTF) $_4$ (NH $_4^+$)[Fe(ox) $_3$](2-Cl-3-FPy) (3)

8 mg BEDT-TTF, 75 mg of (NH $_4$) $_3$ [Fe(ox) $_3$] \cdot 3H $_2$ O, 250 mg of 18-crown-6 and the mixture of 2-Cl-3-FPy (4 mL) with 1,2,4-trichlorobenzene (4 mL) and 96% EtOH (1 mL); $J = 0.9 \mu\text{A}$. Very many small thick crystals were collected from the anode after 2 weeks.

3.1.4. β'' -(BEDT-TTF) $_4$ (NH $_4^+$)[Fe(ox) $_3$](2,6-DCIPy) (4)

A total of 14 mg of BEDT-TTF, 150 mg of (NH $_4$) $_3$ [Fe(ox) $_3$] \cdot 3H $_2$ O, 450 mg of 18-crown-6, 5 g of 2,6-DCIPy were dissolved in the mixture of 30 mL 1,2,4-trichlorobenzene with 3 mL of 96% ethanol. $J = 0.95 \mu\text{A}$. Several thick crystals in the form of plates were collected from the anode after 2 weeks.

3.1.5. β'' -(BEDT-TTF)₄(NH₄⁺)[Fe(ox)₃](2,6-DFPy) (5)

A total of 18 mg of BEDT-TTF, 150 mg of (NH₄)₃Fe(ox)₃, 450 mg of 18-crown-6 were dissolved in the mixture of 15 mL of 2,6-DFPy, 5 mL 1,2,4-trichlorobenzene and 2 mL of 96% ethanol. $J = 0.9 \mu\text{A}$. Several thick crystals in the form of plates were collected from the anode after 6 days.

3.2. Structure

X-ray diffraction analyses of the salts **1–5** were carried out on a CCD Agilent XCalibur diffractometer with an EOS detector (Agilent Technologies UK Ltd., Yarnton, Oxfordshire, England). Data collection, determination and refinement of unit cell parameters were carried out using the CrysAlis PRO program suite [38]. X-ray diffraction data at 100(1) K for the salts **1–5** were collected using MoK α ($\lambda = 0.71073 \text{ \AA}$) radiation. The same single crystal for the salt **1** was used for the data collection at different temperatures. Data at 100(1) K for the experiment **1a**, data at 150(1) K for the experiment **1b**, and data at 240(1) K for the experiment **1c** were seamlessly collected without removing the crystal from the diffractometer.

The structures **1–5** were solved by the direct methods. The positions and thermal parameters of non-hydrogen atoms were refined isotropically and then anisotropically by the full-matrix least-squares method. The positions of the hydrogen atoms were calculated geometrically. The guest molecule was found to be disordered over two positions. The geometry of guest molecule was recovered for salts **1–5** except salt **3**. Guest solvent molecules in salt **3** were refined as a set of separated carbon atoms plus fluorine with released occupancies.

The X-ray crystal structures data have been deposited with the Cambridge Crystallographic Data Center, with reference codes CCDC 2081357 (**1a**), 2081360 (**1b**), 2081356 (**1c**), 2081355 (**2**), 2081361 (**3**), 2081354 (**4**), 2079902 (**5**). All calculations were performed with the SHELX-97 program package [39].

3.3. Conducting Properties

The temperature dependences of the electrical resistance of single crystals were measured using a four-probe technique by a lock-in detector at 20 Hz alternating current $J = 1 \text{ mA}$ in the temperature range (1.4–300 K). Two contacts were attached to each of the two opposite sample surfaces with conducting graphite paste. In the experiment, we have measured the out-of-plane resistance R_{\perp} with the current running perpendicular to the conducting layers. Because of the high anisotropy of the samples, we did not succeed in the measurements of the in-plane sample resistance. The out-of-plane resistivity ρ_{\perp} of the samples was calculated from R_{\perp} taking into account that the out-of-plane current is uniform due to the high sample anisotropy.

4. Conclusions

Crystals of new layered molecular (super)conductors (**1–5**) based on radical cation salts of bis(ethylenedithio)tetrathiafulvalene (BEDT-TTF) with paramagnetic tris(oxalate)metallate anions, β'' -(BEDT-TTF)₄(A⁺)[M³⁺(C₂O₄)₃]G, where M is Fe; A is NH₄⁺; G is an isomer of mono- or dihalopyridine: 2-fluoropyridine (2-FPy) (**1**), 2,3-difluoropyridine (2,3-DFPy) (**2**), 2-chloro-3-fluoropyridine (2-Cl-3-FPy) (**3**), 2,6-dichloropyridine (2,6-DCIPy) (**4**) and 2,6-difluoropyridine (2,6-DFPy) (**5**), belong to the monoclinic group of the large family of (BEDT-TTF)₄(A⁺)[M³⁺(C₂O₄)₃]G crystals. In the structures of these crystals, the conducting layers of BEDT-TTF radical cations alternate with supramolecular insulating anionic layers {A⁺[M³⁺(C₂O₄)₃]G}²⁻. Changing the number of halogen atoms in the “guest” molecule halopyridine (G) as well as their size and mutual arrangement has a significant effect on the structure and conducting properties of the crystals. So, salt **1** (G = 2-FPy) undergoes a structural phase transition from monoclinic to triclinic symmetry in the range 100–150 K. A similar transition in isostructural crystals with G = 2-CIPy and 2-BrPy precedes the superconducting transition [25]. However, crystals **1** show stable metallic properties

down to 1.4 K and do not undergo a superconducting transition. In contrast to **1**, crystals **2–5**, where G are various isomers of dihalopyridine, retain monoclinic symmetry in the entire range of the X-Ray experiment (90–300 K). Crystals **2** and **3**, which contain the asymmetric “guest” molecules (2,3-DFPy and 2-Cl-3-FPy, respectively), exhibit the stable metallic properties down to 1.4 K without a superconducting transition. However, the quality of crystals **2** (R-factor = 4.95%) containing two identical substituents in the pyridine molecule is significantly higher than the quality of crystals **3**, where G contain two different substituents. Unlike all other salts, the salt **3** contains an NH_4^+ cation displaced from the lattice twofold axis and shows an oxalic ligand disorder in the tris(oxalato)ferrate anion (see Section Structure).

Crystals **4** (G = 2,6-DCIPy) and **5** (2,6-DFPy) contain the highly symmetric G molecules. Each of these molecules contains two identical substituents. In this case, there were no problems with the quality of the crystals formed. Crystals **4** demonstrate metallic properties down to 1.4 K, while crystals **5** show the onset of a superconducting transition at 3.1 K. This is the first superconductor among crystals of the $\beta''\text{-(BEDT-TTF)}_4(\text{A}^+)[\text{M}^{3+}(\text{C}_2\text{O}_4)_3]\text{G}$ family containing dihalopyridines or dihalobenzenes as G.

Supplementary Materials: The following are available online at <https://www.mdpi.com/article/10.3390/magnetochemistry7060083/s1>, Figure S1: Molecular structure of crystals **5**, $\beta''\text{-(BEDT-TTF)}_4(\text{NH}_4)[\text{Fe}(\text{C}_2\text{O}_4)_3](2,6\text{-DFPy})$, with atom numbers.

Author Contributions: Idea, methodology, synthesis of crystals, writing sections “Abstract, Introduction, Synthesis, Conclusions”—T.G.P., E.B.Y.; the X-ray experiments—A.A.B., G.V.S.; analysis and description of the X-ray data—A.A.B.; the conductivity measurement on crystals, writing section “Conducting properties”—V.N.Z., L.I.B. All authors have read and agreed to the published version of the manuscript.

Funding: This research was done according to the state tasks of Ministry of Science and Higher Education of the Russian Federation (Grants No. AAAA-A19-119092390079-8 for IPCP RAS and No. 075-00920-20-00 for IMTHPM RAS) and supported by the Russian Foundation for Basic Research (Grant No. 21-52-12027).

Institutional Review Board Statement: Not applicable.

Informed Consent Statement: Not applicable.

Data Availability Statement: The crystallographic data have been deposited with the Cambridge Crystallographic Data Centre (<https://www.ccdc.cam.ac.uk/structures/>), deposition numbers 2079902, 2081354–2081357, 2081360, 2081361. See Section 3.2 for details.

Conflicts of Interest: The authors declare no conflict of interest. The funders had no role in the design of the study; in the collection, analyses, or interpretation of data; in the writing of the manuscript, or in the decision to publish the results.

References

1. Kurmoo, M.; Graham, A.W.; Day, P.; Coles, S.J.; Hursthouse, M.B.; Caufield, J.L.; Singleton, J.; Pratt, F.L.; Hayes, W.; Ducasse, L.; et al. Superconducting and Semiconducting Magnetic Charge Transfer Salts: $(\text{BEDT-TTF})_4\text{AFe}(\text{C}_2\text{O}_4)_3\text{C}_6\text{H}_5\text{CN}$; A = H_2O , K, NH_4 . *J. Am. Chem. Soc.* **1995**, *117*, 12209–12217. [[CrossRef](#)]
2. Martin, L.; Turner, S.S.; Day, P.; Mabbs, F.E.; McInnes, J.L. New molecular superconductor containing paramagnetic chromium (III) ions. *Chem. Commun.* **1997**, 1367–1368. [[CrossRef](#)]
3. Turner, S.S.; Day, P.; Abdul Malik, K.M.; Hursthouse, M.B.; Teat, S.J.; MacLean, E.J.; Martin, L.; French, S.A. Effect of Included Solvent Molecules on the Physical Properties of the Paramagnetic Charge Transfer Salts $\beta''\text{-(BEDT-TTF)}_4[(\text{H}_3\text{O})\text{Fe}(\text{C}_2\text{O}_4)_3]\text{Solvent}$ (BEDT-TTF = Bis(ethylenedithio)tetrathiafulvalene). *Inorg. Chem.* **1999**, *38*, 3543–3549. [[CrossRef](#)]
4. Martin, L.; Turner, S.S.; Day, P.; Guionneau, P.; Howard, J.A.K.; Hibbs, D.E.; Light, M.E.; Hursthouse, M.B.; Uruichi, M.; Yakushi, K. Crystal Chemistry and Physical Properties of Superconducting and Semiconducting Charge Transfer Salts of the Type $(\text{BEDT-TTF})_4[\text{A}^1\text{M}^{\text{III}}(\text{C}_2\text{O}_4)_3]\text{PhCN}$ ($\text{A}^1 = \text{H}_3\text{O}$, NH_4 , K; $\text{M}^{\text{III}} = \text{Cr}$, Fe, Co, Al; BEDT-TTF = Bis(ethylenedithio)tetrathiafulvalene). *Inorg. Chem.* **2001**, *40*, 1363–1371. [[CrossRef](#)]
5. Rashid, S.; Turner, S.S.; Le Pevelen, D.; Day, P.; Light, M.E.; Hursthouse, M.B.; Firth, S.; Clark, R.J.H. $\beta''\text{-(BEDT-TTF)}_4[(\text{H}_3\text{O})\text{Cr}(\text{C}_2\text{O}_4)_3]\text{CH}_2\text{Cl}_2$: Effect of Included Solvent on the Structure and Properties of a Conducting Molecular Charge-Transfer Salt. *Inorg. Chem.* **2001**, *40*, 5304–5306. [[CrossRef](#)]

6. Rashid, S.; Turner, S.S.; Day, P.; Howard, J.A.K.; Guionneau, P.; McInnes, E.J.L.; Mabbs, F.E.; Clark, R.J.H.; Firth, S.; Biggse, T. New superconducting charge-transfer salts (BEDTTF)₄[AM(C₂O₄)₃]C₆H₅NO₂ (A = H₃O or NH₄, M = Cr or Fe, BEDT-TTF = bis(ethylenedithio)tetrathiafulvalene). Novel charge transfer salts of BEDT-TTF with metal oxalate counterions. *J. Mater. Chem.* **2001**, *11*, 2095–2101. [[CrossRef](#)]
7. Rashid, S.S.; Turner, P.; Day, M.E.; Light, M.B.; Hursthouse, P. Guionneau. *Synth. Met.* **2001**, *120*, 985–986. [[CrossRef](#)]
8. Akutsu, H.; Akutsu-Sato, A.; Turner, S.S.; Le Pevelen, D.; Day, P.; Laukhin, V.; Klehe, A.-K.; Singleton, J.; Tocher, D.A.; Probert, M.R.; et al. Effect of Included Guest Molecules on the Normal State Conductivity and Superconductivity of β''-(ET)₄[(H₃O)Ga(C₂O₄)₃]G (G = Pyridine, Nitrobenzene). *J. Am. Chem. Soc.* **2002**, *124*, 12430–12431. [[CrossRef](#)]
9. Prokhorova, T.G.; Khasanov, S.S.; Zorina, L.V.; Buravov, L.I.; Tkacheva, V.A.; Baskakov, A.A.; Morgunov, R.B.; Gener, M.; Canadell, E.; Shibaeva, R.P.; et al. Molecular Metals Based on BEDT-TTF Radical Cation Salts with Magnetic Metal Oxalates as Counterions: β''-(BEDT-TTF)₄A[M(C₂O₄)₃]DMF (A = K⁺, NH₄⁺; M = Fe^{III}, Cr^{III}). *Adv. Func. Mater.* **2003**, *13*, 403–411. [[CrossRef](#)]
10. Coldea, A.I.; Bangura, A.F.; Singleton, J.; Ardavan, A.; Akutsu-Sato, A.; Akutsu, H.; Turner, S.S.; Day, P. Fermi-surface topology and the effects of intrinsic disorder in a class of charge-transfer salts containing magnetic ions: β''-(BEDT-TTF)₄[(H₃O)M(C₂O₄)₃]Y (M = Ga, Cr, Fe; Y = C₅H₅N). *Phys. Rev. B* **2004**, *69*, 085112. [[CrossRef](#)]
11. Akutsu, H.; Akutsu-Sato, A.; Turner, S.S.; Day, P.; Canadell, E.; Firth, S.; Clark, R.J.N.; Yamada, J.; Nakatsuji, S. Superstructures of donor packing arrangements in a series of molecular charge transfer salts. *Chem. Commun.* **2004**, 18–19. [[CrossRef](#)]
12. Audouard, A.; Laukhin, V.N.; Brossard, L.; Prokhorova, T.G.; Yagubskii, E.B.; Canadell, E. Combination frequencies of magnetic oscillations in β''-(BEDT-TTF)₄(NH₄)[(Fe(C₂O₄)₃]DMF. *Phys. Rev. B* **2004**, *69*, 144523. [[CrossRef](#)]
13. Akutsu-Saito, A.; Kobayashi, A.; Mori, T.; Akutsu, H.; Yamada, J.; Nakatsuji, S.; Turner, S.S.; Day, P.; Tocher, D.A.; Light, M.E.; et al. Structures and Physical Properties of New β''-BEDT-TTF Tris-Oxalatometallate (III) Salts Containing Chlorobenzene and Halomethane Guest Molecules. *Synth. Met.* **2005**, *152*, 373–376. [[CrossRef](#)]
14. Coronado, E.; Curelli, S.; Giménez-Saiz, C.; Gómez-García, C.J. New magnetic conductors and superconductors based on BEDT-TTF and BEDS-TTF. *Synth. Met.* **2005**, *154*, 245–248. [[CrossRef](#)]
15. Coronado, E.; Curelli, S.; Giménez-Saiz, C.; Gómez-García, C.J. A novel paramagnetic molecular superconductor formed by bis(ethylenedithio)tetrathiafulvalene, tris(oxalato)ferrate(III) anions and bromobenzene as guest molecule: (ET)₄[(H₃O)Fe(C₂O₄)₃]C₆H₅Br. *J. Mater. Chem.* **2005**, *15*, 1429–1436. [[CrossRef](#)]
16. Akutsu-Sato, A.; Akutsu, H.; Yamada, J.; Nakatsuji, S.; Turner, S.S.; Day, P. Suppression of superconductivity in a molecular charge transfer salt by changing quest molecule: β''-(BEDT-TTF)₄[(H₃O)Fe(C₂O₄)₃](C₆H₅CN)_x(C₅H₅N)_{1-x}. *J. Mater. Chem.* **2007**, *17*, 2497–2499. [[CrossRef](#)]
17. Zorina, L.V.; Prokhorova, T.G.; Simonov, S.V.; Khasanov, S.S.; Shibaeva, R.P.; Manakov, A.I.; Zverev, V.N.; Buravov, L.I.; Yagubskii, E.B. Structure and Magnetotransport Properties of the New Quasi-Two-Dimensional Molecular Metal β''-(BEDT-TTF)₄H₃O[Fe(C₂O₄)₃]C₆H₄Cl₂. *JETP* **2008**, *106*, 347–354. [[CrossRef](#)]
18. Martin, L.; Day, P.; Akutsu, H.; Yamada, J.; Nakatsuji, S.; Clegg, W.; Harrington, R.W.; Horton, P.N.; Hursthouse, M.B.; McMillan, P.; et al. Metallic molecular crystals containing chiral or racemic guest molecules. *CrystEngComm* **2007**, *9*, 865–867. [[CrossRef](#)]
19. Prokhorova, T.G.; Buravov, L.I.; Yagubskii, E.B.; Zorina, L.V.; Khasanov, S.S.; Simonov, S.V.; Shibaeva, R.P.; Korobenko, A.V.; Zverev, V.N. Effect of electrocrystallization medium on quality, structural features, and conducting properties of single crystals of the (BEDT-TTF)₄A^I[Fe^{III}(C₂O₄)₃]G family. *CrystEngComm* **2011**, *13*, 537–545. [[CrossRef](#)]
20. Zorina, L.V.; Khasanov, S.S.; Simonov, S.V.; Shibaeva, R.P.; Zverev, V.N.; Canadell, E.; Prokhorova, T.G.; Yagubskii, E.B. Coexistence of two donor packing motifs in the stable molecular metal α'-pseudo-κ'-(BEDT-TTF)₄(H₃O)[Fe(C₂O₄)₃]C₆H₄Br₂. *CrystEngComm* **2011**, *13*, 2430–2438. [[CrossRef](#)]
21. Coronado, E.; Curreli, S.; Giménez-Saiz, C.; Gómez-García, C.J. The Series of Molecular Conductors and Superconductors ET₄[AFe(C₂O₄)₃]·PhX (ET = bis(ethylenedithio)tetrathiafulvalene; (C₂O₄)²⁻ = oxalate; A⁺ = H₃O⁺, K⁺; X = F, Cl, Br, and I): Influence of the Halobenzene Guest Molecules on the Crystal Structure and Superconducting Properties. *Inorg. Chem.* **2012**, *51*, 1111–1126. [[PubMed](#)]
22. Zorina, L.V.; Khasanov, S.S.; Simonov, S.V.; Shibaeva, R.P.; Bulanchuk, P.O.; Zverev, V.N.; Canadell, E.; Prokhorova, T.G.; Yagubskii, E.B. Structural phase transition in the β''-(BEDT-TTF)₄H₃O[Fe(C₂O₄)₃]·G crystals (where G is a guest solvent molecule). *CrystEngComm* **2012**, *14*, 460–465. [[CrossRef](#)]
23. Prokhorova, T.G.; Zorina, L.V.; Simonov, S.V.; Zverev, V.N.; Canadell, E.; Shibaeva, R.P.; Yagubskii, E.B. The first molecular superconductor based on BEDT-TTF radical cation salt with paramagnetic tris(oxalato)ruthenate anion. *CrystEngComm* **2013**, *15*, 7048–7055. [[CrossRef](#)]
24. Prokhorova, T.G.; Buravov, L.I.; Yagubskii, E.B.; Zorina, L.V.; Simonov, S.V.; Shibaeva, R.P.; Zverev, V.N. New metallic bi-and monolayered radical cation salts based on BEDT-TTF with tris(oxalato)gallate anion. *Eur. J. Inorg. Chem.* **2014**, *2014*, 3933–3940. [[CrossRef](#)]
25. Prokhorova, T.G.; Buravov, L.I.; Yagubskii, E.B.; Zorina, L.V.; Simonov, S.V.; Zverev, V.N.; Shibaeva, R.P.; Canadell, E. Effect of the halopyridine guest molecules (G) on the structure and (super)conducting properties of the β''-(BEDT-TTF)₄(H₃O)[Fe(C₂O₄)₃]G crystals. *Eur. J. Inorg. Chem.* **2015**, *2015*, 5611–5620. [[CrossRef](#)]
26. Martin, L.; Morrith, A.L.; Lopez, J.R.; Nakazawa, Y.; Akutsu, H.; Imajo, S.; Ihara, Y.; Zhang, B.; Zhange, Y.; Guof, Y. Molecular conductors from bis(ethylenedithio)tetrathiafulvalene with tris(oxalato)rhodate. *Dalt. Trans.* **2017**, *46*, 9542–9548. [[CrossRef](#)] [[PubMed](#)]

27. Prokhorova, T.G.; Yagubskii, E.B. Organic conductors and superconductors based on bis(ethylenedithio)tetrathiafulvalene radical cation salts with supramolecular tris(oxalato)metallate anions. *Russ. Chem. Rev.* **2017**, *86*, 164–180. [[CrossRef](#)]
28. Prokhorova, T.G.; Yagubskii, E.B.; Zorina, L.V.; Simonov, S.V.; Zverev, V.N.; Shibaeva, R.P.; Buravov, L.I. Specific structural disorder in an anion layer and its influence on conducting properties of new crystals of the (BEDT-TTF)₄A⁺[M³⁺(ox)₃]G family, where G is 2-halopyridine; M is Cr, Ga; A⁺ is [K_{0.8}(H₃O)_{0.2}]⁺. *Crystals* **2018**, *8*, 92. [[CrossRef](#)]
29. Martin, L. Molecular conductors of BEDT-TTF with tris(oxalato)metallate anions. *Coord. Chem. Rev.* **2018**, *376*, 277–291. [[CrossRef](#)]
30. Mori, T. Structural Genealogy of BEDT-TTF-Based Organic Conductors I. Parallel Molecules: β and β'' Phases. *Bull. Chem. Soc. Jpn.* **1998**, *71*, 2509–2526. [[CrossRef](#)]
31. Mori, T.; Mori, H.; Tanaka, S. Structural Genealogy of BEDT-TTF-Based Organic Conductors II. Inclined Molecules: θ , α , and κ Phases. *Bull. Chem. Soc. Jpn.* **1999**, *72*, 179–197. [[CrossRef](#)]
32. Olejniczak, I.; Frackowiak, A.; Swietlik, R.; Prokhorova, T.G.; Yagubskii, E.B. Charge Fluctuations and Ethylene-Group-Ordering Transition in β'' -(BEDT-TF)₄[(H₃O)Fe(C₂O₄)₃]Y Molecular Charge-Transfer Salts. *ChemPhysChem* **2013**, *14*, 3925–3935. [[CrossRef](#)]
33. Merino, J.; McKenzie, R.H. Superconductivity Mediated by Charge Fluctuations in Layered Molecular Crystals. *Phys. Rev. Lett.* **2001**, *87*, 237002. [[CrossRef](#)]
34. Martin, L.; Morritt, A.; Lopez, J.R.; Akutsu, H.; Nakazawa, Y.; Imajo, S.; Ihara, Y. Ambient-pressure molecular superconductor with a superlattice containing layers of tris(oxalato)rhodate enantiomers and 18-crown-6. *Inorg. Chem.* **2017**, *56*, 717–720. [[CrossRef](#)]
35. Martin, L.; Lopez, J.R.; Nakazawa, Y.; Imajo, S. Bulk Kosterlitz–Thouless Type Molecular Superconductor β'' -(BEDT-TTF)₂[(H₂O)(NH₄)₂Cr(C₂O₄)₃]18-crown-6. *Inorg. Chem.* **2017**, *56*, 14045–14052. [[CrossRef](#)] [[PubMed](#)]
36. Morritt, A.L.; Lopez, J.R.; Blundell, T.J.; Canadell, E.; Akutsu, H.; Nakazawa, Y.; Imajo, S.; Martin, L. 2D Molecular Superconductor to Insulator Transition in the β'' -(BEDT-TTF)₂[(H₂O)(NH₄)₂M(C₂O₄)₃]·18-crown-6 Series (M = Rh, Cr, Ru, Ir). *Inorg. Chem.* **2019**, *58*, 10656–10664. [[CrossRef](#)] [[PubMed](#)]
37. Guionneau, P.; Kepert, C.J.; Chasseau, D.; Truter, M.R.; Day, P. Determining the charge distribution in BEDT-TTP salts. *Synth. Met.* **1997**, *86*, 1973–1974. [[CrossRef](#)]
38. Agilent. *CrysAlis PRO Version 171.35.19*; Agilent Technologies UK Ltd.: Oxfordshire, UK, 2011.
39. Sheldrick, G.M. *SHELXL-97. Program for Crystal Structure Refinement*; University of Göttingen: Göttingen, Germany, 1997.